Structures and electronic properties of small carbon nanotube tori

Dong-Hwa Oh,[1] Jung Mee Park,[2] and Kwang S. Kim[1,2*]
[1]*National Creative Research Initiative Center for Superfunctional Materials, Pohang 790-784, Korea*
[2]*Department of Chemistry, Pohang University of Science and Technology, Pohang 790-784, Korea*
(Received 6 April 2000)

Fullerenes and nanotubes are promising candidates in the development of nanodevices. Recently, a form of carbon nanotube torus structures has been observed. In this regard, we have investigated the geometries, electronic structures, and energetics of small carbon nanotube tori, using both the tight-binding and semiempirical quantum chemical approaches. It is shown that D_{5d} nanotube tori behave like semiconductors, while D_{6h} nanotube tori exhibit metal (or metal-like) characteristics similar to bent nanotubes. We show that the D_{5d} nanotube tori, which are as stable as the corresponding fullerenes, are energetically more favored than the corresponding nanotubes. In particular, the pentagons of the D_{5d} nanotube tori are less deformed than those of bent nanotubes and D_{6h} nanotube tori. This indicates that such small nanotube tori could be observed under optimal kinetic-driven conditions and eventually utilized as nanodevices.

Fullerenes[1] and carbon nanotubes (C tubes) (Ref. 2) have attracted a lot of interest because these fascinating carbon clusters have shown great promise in the development of futuristic nanodevices and nanomaterials.[3] Recently, the groups of Smalley[4] and Avouris[5] have reported rings of C tubes (carbon nanotube tori with radius of $\sim$300 nm), using scanning force and transmission electron microscopy.

The structures of these carbon nanotori (C tori) were theoretically suggested by Dunlap,[6] followed by Itoh *et al.*[7] Using a tight-binding (TB) model,[8] Dunlap introduced C tori of D_{6h} symmetry made up of armchair and zigzag C tube segments. On the other hand, Itoh *et al.* investigated C-tori of D_{5d} symmetry with large ratios of width to diameter, based on a Goldberg transformation[9] using an empirical potential.[10] While the D_{6h} C tori contain 12 pairs of pentagons and heptagons, the corresponding D_{5d} C tori contain ten pairs. The heptagons reflect surfaces with negative curvature.[11] Another structural model for C tori can be constructed by bending and connecting both ends without introducing pentagons and heptagons. In such cases the tube lengths are extremely long and hence can be simply to be a special case of a very long C tube.

Previous studies of C tori by Dunlap and Itoh *et al.* were based on different calculational schemes, so a direct comparison of the properties of different types of C tori cannot be made. Furthermore, the electronic structure of D_{5d} C tori have yet not been reported because the structures were investigated with simple empirical potentials. Therefore, the focus of the paper is to compare the properties of these different C tori using theoretical approaches employing TB method with parameters of Xu *et al.*[12] and the semiempirical quantum chemical parametrized method 3 (PM3).[13] The stabilities of various C tori are compared with those of icosahedral fullerenes (Fuls) and single wall C tubes. Both the TB and PM3 methods show consistent results.

We have investigated various types of carbon clusters C_N, viz., C tori of D_{5d} symmetry of Itoh *et al.* (C_{120}, C_{360}, and C_{480}), Dunlap's C tori of D_{6h} symmetry, and other types of C tori (Fig. 1). Dunlap's C tori can be classified as types n wherein segments of (n,n) armchair and $(2n,0)$ zigzag tubes are connected [C_{324} and C_{540} (type III) and C_{480}, C_{576}, and C_{768} (type IV)]. New types (type n') of C tori can have various types of symmetry (D_{5h}, D_{6h}, and D_{7h}) wherein segments of (n,n) armchair and $(2n+1,0)$ zigzag tubes are connected. We have noted that Dunlap's type n can also be extended to have other symmetries (D_{5h}, D_{7h}), but its structure and property are not very different from those of the type-n' C tori, so we do not include it in the subsequent discussion. Instead, Fuls (C_{60}, C_{180}, C_{240}, and C_{540}), armchair (n,n), and zigzag $(n,0)$ C tubes as well as the carbon graphite sheet were investigated for comparison. All these structures were completely optimized using both theoretical approaches. The structural parameters (average radius r_{av}, cylindrical cross section radius r_{cyl}), average value of the energies per carbon atom (E_c), and energy band gaps (E_{gap}) of Fuls, C tori, C tubes, and graphite are listed in Table I. Figure 2 shows the dependence of E_c on the number of carbon atoms (N) for various types of carbon clusters of Fuls and C tori, which are compared with C tubes and graphite sheet. Since the reference energies of TB and PM3 methods are different, the E_c's of TB are compared with those of PM3 with an offset value.

In the case of Fuls, as N increases, E_c gets lowered, and E_{gap} decreases toward the values of graphite ($E_c=-8.07$ eV, $E_{\mathrm{gap}}=0$ eV). The dependence of E_c on N (for $N\gg 1$) follows the classical theory of elasticity,[14] $\Delta E_c=(-11.92+8.28\ln N)/N$, where ΔE_c is the difference in E_c between Ful and graphite.

The D_{5d} C tori show a trend in energy similar to that of Fuls; i.e., with increasing N, E_c gets lowered, and E_{gap} decreases toward the values of graphite. The dependence of E_c on N also follows the classical theory of elasticity, $\Delta E_c=(-9.27+14.14\ln N)/N$.

On the other hand, E_c's of D_{6h} C tori mainly depend on the types of C-tube segments connected together, but only slightly on the length of C-tube segments. C_{324} and C_{540} are made up of (3,3) and (6,0) C-tube segments (type III), while C_{480}, C_{576}, and C_{768} are made up (4,4) and (8,0) C-tube segments (type IV). In these cases, the values of E_c and E_{gap} highly depend on the type n, whereas for a given type, E_c is

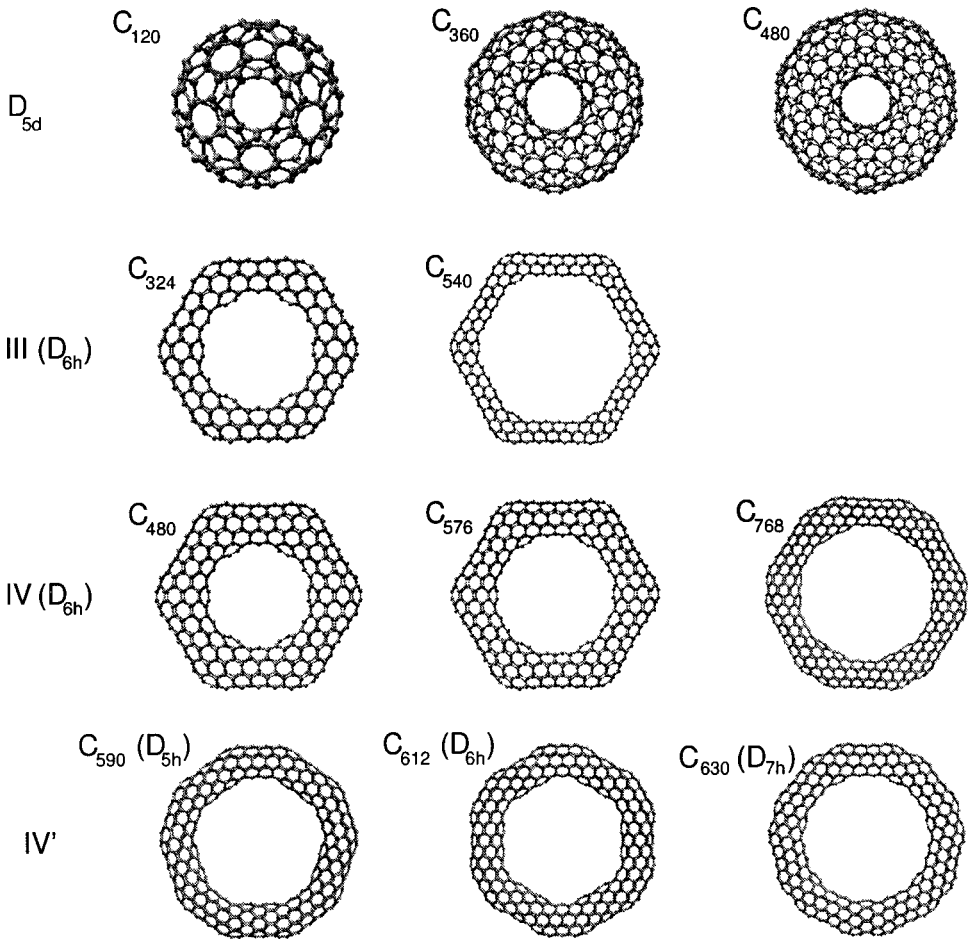

FIG. 1. Optimized structures of various types of carbon nanotube tori.

almost constant regardless of N, and E_{gap} changes little with respect to N. This indicates that the properties of D_{6h} C tori are inherited from the composing C tube components. The results indicate that the E_c of D_{6h} C tori is around (or only slightly higher than) the weight average value of the two different C-tube components (armchair and zigzag tubes), since the energy increase due to adjoined parts is only a small fraction of the total energy contribution. Since E_c's of (6,0) and (3,3) C tubes are, respectively, -7.71 and -7.61 eV, the E_c's of type-III E_{6h} C tori (C_{324}, C_{540}, ...) are -7.66 eV (the average value of two C-tube segments which have almost the same weight). Similarly, the E_c's of type-IV D_{6h} C tori (C_{480}, C_{576}, C_{768}, ...) [which are composed of (8,0) and (4,4) C-tube segments whose E_c's are -7.84 and -7.81 eV, respectively] are around -7.8 eV. Thus, one can expect that the E_c's of type V of D_{6h} C tori [which are composed of (10,0) and (5,5) C-tube segments whose E_c's are -7.96 and -7.89 eV] are around -7.9 eV. Of course, slightly different C tori can be made up certain short C-tube segments and another long C-tube segments. In this case, the E_c could be around the weight average value of two C-tube segments. Regardless of symmetry, E_c's of type n' C tori are similar to that those of type n (D_{6h}). However, in type n', the pentagonal shape (D_{5h}) tends to be slightly more favored energetically.

Figure 3 shows the radial distribution functions (RDFs), the bond angle distribution functions (ADFs), and the local energy distribution of selected carbon clusters [C_{768}(D_{6h}; IV), C_{480}(D_{5d}), and C_{60} (Ful)]. In RDFs [Fig. 3(a)], the D_{5d} C torus has a broad peak, while the D_{6h} torus have a few sharp peaks. In both cases, 1.42 Å peak (which is present in graphite) is dominant. From these peaks, we expect that the D_{5d} torus shows gradual deformation from graphite, while the D_{6h} torus shows abrupt deformation at the joint regions.

In ADFs [Fig. 3(b)], the D_{5d} torus shows a broad peak near $\sim 120°$ and small peaks near $\sim 108°$ and $\sim 128°$ corresponding to pentagons and heptagons, respectively. The D_{6h} torus shows sharp peaks near 120° and small broadly split peaks near $\sim 108°$ in the joint regions between different C-tube segments, indicating highly deformed pentagons. Excluding the joint regions, the electronic structure of D_{6h} C torus retains some characteristics of C tubes. On the other hand, the small and gradual deformation in the D_{5d} C torus results in a larger E_{gap} than the abrupt deformation in the D_{6h} C torus.

The local energy distribution [Fig. 3(c)] shows that the pentagons of the D_{6h} torus are highly deformed and less stable than those of the D_{5d} torus. In the D_{6h} C torus, the local energies of carbon atoms are nearly same as those of the corresponding C tube except for carbon atoms near the interface between the C-tube segments. In the D_{5d} C torus, the local energies are much less spread out than those in the D_{6h} torus. Thus, in the case of D_{5d} C tori, the local energy distribution (for carbon atom) is rather uniform, while in the case of D_{6h} C tori, the carbon atoms in the junction regions between two different C-tube segments have very different electronic properties from many other carbon atoms. The uniform distribution of local energy per carbon atom in D_{5d}

TABLE I. Average radius [$r_{av}(r_{cyl})$ in Å], total energy per carbon atom (E_c in eV), and HOMO-LUMO gaps (E_{gap} in eV) of Fuls, C tori, and C tubes.

		TB			PM3	
Type	N	$r_{av}(r_{cyl})$	E_c	E_{gap}	$r_{av}(r_{cyl})$	E_c
Fullerene						
	60	3.595	−7.70	1.56	3.546	0.59
	180	6.156	−7.89	1.18	6.121	0.32
	240	7.133	−7.93	1.02	7.055	0.29
	540	10.636	−7.98	0.72	—	—
Nanotube torus						
D_{5d}	120	4.744(2.017)	−7.58	0.93	4.716(2.004)	0.68
	360	8.096(3.447)	−7.86	0.32	8.048(3.422)	0.35
	480	9.310(4.025)	−7.91	0.32	9.254(4.000)	0.30
D_{6h} (III)	324	10.265(2.245)	−7.66	0.04	10.249(2.224)	0.60
	540	16.950(2.263)	−7.66	0.00	16.814(2.254)	0.63
D_{6h} (IV)	480	11.608(2.911)	−7.80	0.27	11.564(2.890)	0.43
	576	14.878(2.615)	−7.81	0.15	—	—
	768	17.777(2.991)	−7.82	0.04	—	—
D_{5h} (IV′)	590	14.662(2.806)	−7.81	0.25	—	—
D_{6h} (IV′)	612	15.083(2.816)	−7.80	0.01	—	—
D_{7h} (IV′)	630	15.559(2.788)	−7.76	0.32	—	—
Nanotube						
(10,10)	∞	6.780	−8.01	0.00	—	—
(5,5)	∞	3.390	−7.89	0.00	—	—
(4,4)	∞	2.712	−7.81	0.00	—	—
(3,3)	∞	2.034	−7.61	0.00	—	—
(10,0)	∞	3.914	−7.90	0.59	—	—
(9,0)	∞	3.523	−7.86	0.09	—	—
(8,0)	∞	3.132	−7.84	0.99	—	—
(6,0)	∞	2.347	−7.71	0.20	—	—
Graphite	∞	—	−8.07	0.00	—	—

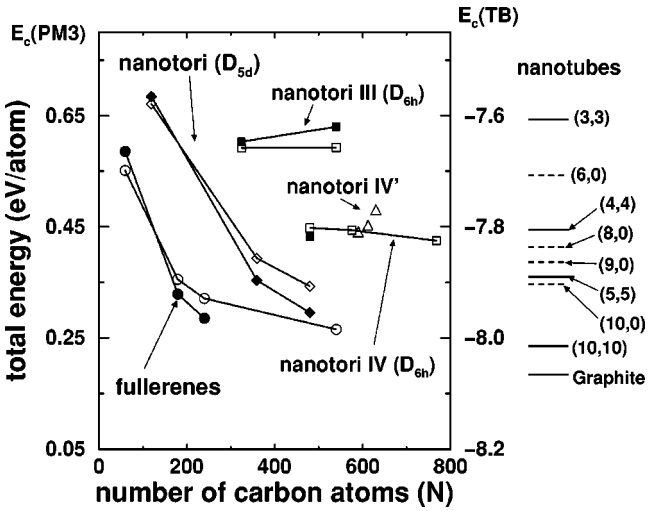

FIG. 2. Dependence of the energy per carbon atom on the number of carbon atoms for icosahedral fullerenes and carbon nanotube tori of D_{5d} and D_{6h} symmetries. The energies of carbon nanotubes and graphite are also given for comparison. The PM3 and TB values are represented by solid and open symbols, respectively.

C tori would make the pentagons and heptagons frontier orbitals describing the large band gap. Thus these C tori behave like a semiconductor.

Overlaying two E_{gap}'s of two C tubes comprising a C tori tends to make the E_{gap} of a torus smaller than the minimum of two E_{gap}'s (often much smaller in the case of mismatched overlaying band gaps). The D_{5d} C tori behave like a semiconductor, while the E_{gap}'s decrease with increasing N. The E_{gap}'s of D_{6h} C tori reflect those of their composing C-tube components. Since the E_{gap}'s of (k,k) and $(3k,0)$ C tubes (k: integer) are ~ 0 eV,[15] the D_{6h} C tori of types $3k$ and $(3k+1)'$ are expected to be metallic. Indeed, the type-III and -IV′ D_{6h} C tori are predicted to be metallic ($E_{gap} \simeq 0$ eV). The type-IV D_{6h} C tori are semiconductor and metallike (E_{gap}'s of C_{480}, C_{576}, and C_{768} are 0.27, 0.15, and 0.04 eV, respectively). D_{6h} C tori tend to show smaller band gaps with increasing size due to the structural approach toward the graphitelike structure. For type IV′, $C_{590}(D_{5h})$, $C_{612}(D_{6h})$, and $C_{630}(D_{7h})$ C tori show E_{gap}'s of 0.25, 0.01, and 0.32 eV, respectively.

Figure 4 shows the density of states and local density of states of pentagon and heptagon rings of $C_{480}(D_{5d})$, C_{768} (IV; D_{6h}), and C_{590}(IV′; D_{5h}), and C_{630}(IV′; D_{7h}). In the

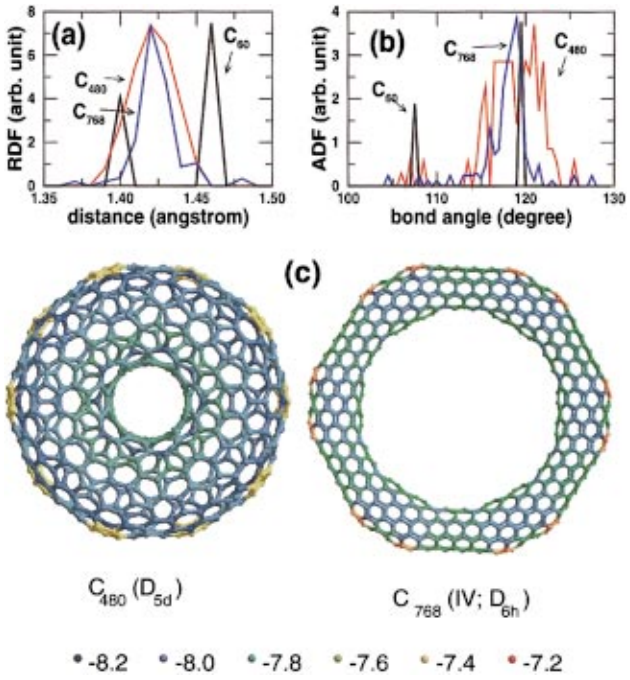

FIG. 3. (Color) (a) Radial distribution functions for the nearest neighbors; (b) bond angle distribution functions of $C_{768}(D_{6h}$; IV), $C_{480}(D_{5h})$, and C_{60} (Fuls), which are represented in blue, red, and black lines, respectively; (c) local atomic energy distributions of C_{768} and C_{480}, wherein the most stable and unstable atoms are indicated as violet and red colors, respectively, while other atomic energies are represented in the order of the rainbow colors (units in eV).

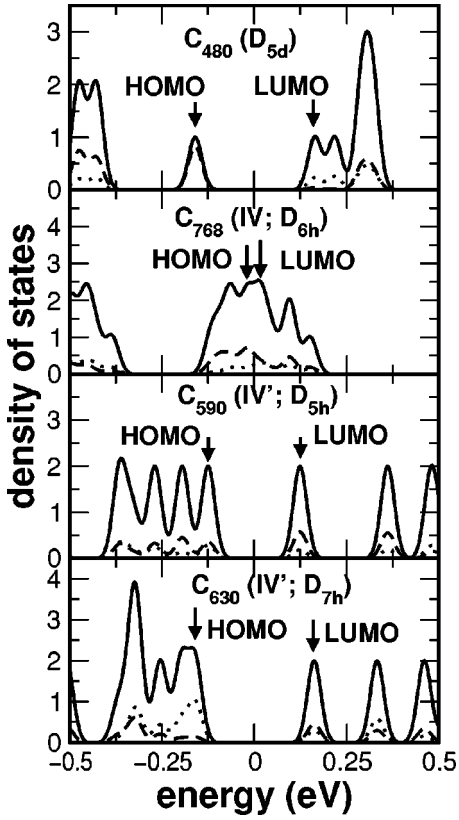

FIG. 4. Density of states near frontier orbitals (HOMO and LUMO) for $C_{480}(D_{5d})$, C_{768} (IV; D_{6h}), C_{590} (IV′; D_{5h}), and C_{630} (IV′; D_{7h}). Dotted and dashed lines represent local densities of states of pentagon and heptagon rings, respectively, while solid lines represent the total density of states.

$C_{480}(D_{5d})$ torus, the highest occupied molecular orbit (HOMO) is almost fully described by atomic orbitals (AOs) of heptagon rings, while the lowest unoccupied molecular orbit (LUMO) by pentagon rings and some of their neighbor atoms. The C_{630}(IV′; D_{7h}) torus shows that the HOMO comprises mostly AOs of pentagon rings, while the LUMO comprises mostly AOs of heptagon rings. Thus, in cases of D_{5d} and D_{7h} tori, the frontier orbitals of the HOMO and LUMO are described mostly by the AOs of pentagons and hexagons, so that the distinction between HOMO and LUMO densities is very clear. This results in an opening of E_{gap} for D_{5d} (and D_{5h}) and D_{7h}. On the other hand, in the C_{768} (IV; D_{6h}) torus, the frontier orbitals of the HOMO and LUMO are mostly described by the AOs of hexagons, so that the distribution between the HOMO and LUMO densities is not noticeable, and the E_{gap} is negligible, resulting in metal characteristics. However, a clearer understanding of these interesting phenomena would be needed with further study.

Since bent C tubes have often been seen in many experiments, Dunlap's C tori of D_{6h} symmetry are found to be particularly interesting, and his work would be useful since the E_{gap}'s of D_{6h} C tori can be predicted from the C tubes bent by 60°. On the other hand, D_{5d} C tori are energetically more stable than other C tori (joined by C tube segments) and C-tubes, and almost as stable as Fuls. This indicates that small D_{5d} C tori could be made under optimal kinetic-driven conditions, as various Fuls and bent C tubes have been observed. The small C tori could eventually be utilized as useful nanodevices such as nanosolenoids and nanotransformers.

This work was supported by MOST/KISTEP(CRI).

*Corresponding author.

[1] H. W. Kroto *et al.*, Nature (London) **318**, 162 (1985).
[2] S. Iijima, Nature (London) **354**, 56 (1991).
[3] Sander J. Tans *et al.*, Nature (London) **386**, 474 (1997); Walt A. de Heer *et al.*, Science **270**, 1179 (1995); A. G. Rinzler *et al.*, *ibid.* **269**, 1550 (1995); A. C. Dillon *et al.*, Nature (London) **386**, 377 (1997).
[4] Jie Liu *et al.*, Nature (London) **385**, 780 (1997).
[5] Richard Martel *et al.*, Nature (London) **398**, 299 (1999).
[6] B. I. Dunlap, Phys. Rev. B **46**, 1933 (1992).
[7] Satoshi Itoh *et al.*, Phys. Rev. B **47**, 1703 (1993); *ibid.* **47**, 12 908 (1993).
[8] D. H. Robertson *et al.*, Phys. Rev. B **45**, 12 592 (1992).
[9] M. Goldberg, Tohoku Math. J. **43**, 104 (1937); P. W. Fowler, Chem. Phys. Lett. **131**, 444 (1986).
[10] F. H. Stillinger and T. A. Weber, Phys. Rev. B **31**, 5262 (1985); **33**, 1451(E) (1986).
[11] A. L. Mackay and H. Terrones, Nature (London) **352**, 762 (1991); T. Lenosky *et al.*, *ibid.* **355**, 333 (1992); D. Vanderbilt and J. Tersoff, Phys. Rev. Lett. **68**, 511 (1992).
[12] C. H. Xu *et al.*, J. Phys.: Condens. Matter **4**, 6047 (1992).
[13] J. J. P. Stewart, J. Comput. Chem. **10**, 209 (1998); **10**, 220 (1998).
[14] J. Tersoff, Phys. Rev. B **46**, 15 546 (1992); Satoshi Itoh, Pablo Ordejön *et al.*, *ibid.* **53**, 2132 (1996).
[15] N. Hamada *et al.*, Phys. Rev. Lett. **68**, 1579 (1992).